THE JOURNAL OF BIOLOGICAL CHEMISTRY VOL. 283, NO. 35, pp. 24145–24154, August 29, 2008

Phosphorylation of the cAMP-dependent Protein Kinase (PKA) Regulatory Subunit Modulates PKA-AKAP Interaction, Substrate Phosphorylation, and Calcium Signaling in Cardiac Cells*[S]

Received for publication, March 21, 2008, and in revised form, June 9, 2008 Published, JBC Papers in Press, June 12, 2008, DOI 10.1074/jbc.M802278200

Sabrina Manni[‡], Joseph H. Mauban[‡], Christopher W. Ward[§], and Meredith Bond[‡1]

From the Departments of [‡]Physiology, School of Medicine, and [§]Organizational System and Adult Health, School of Nursing, University of Maryland Baltimore, Baltimore, Maryland 21201

Subcellular compartmentalization of the cAMP-dependent protein kinase (PKA) by protein kinase A-anchoring proteins (AKAPs) facilitates local protein phosphorylation. However, little is known about how PKA targeting to AKAPs is regulated in the intact cell. PKA binds to an amphipathic helical region of AKAPs via an N-terminal domain of the regulatory subunit. I*n vitro* studies showed that autophosphorylation of type II regulatory subunit (RII) can alter its affinity for AKAPs and the catalytic subunit (PKA_{cat}). We now investigate whether phosphorylation of serine 96 on RII regulates PKA targeting to AKAPs, downstream substrate phosphorylation and calcium cycling in primary cultured cardiomyocytes. We demonstrated that, whereas there is basal phosphorylation of RII subunits, persistent maximal activation of PKA results in a phosphatase-dependent loss of RII phosphorylation. To investigate the functional effects of RII phosphorylation, we constructed adenoviral vectors incorporating mutants which mimic phosphorylated (RIIS96D), nonphosphorylated (RIIS96A) RII, or wild-type (WT) RII and performed adenoviral infection of neonatal rat cardiomyocytes. Coimmunoprecipitation showed that more AKAP15/18 was pulled down by the phosphomimic, RIIS96D, than RIIS96A. Phosphorylation of phospholamban and ryanodine receptor was significantly increased in cells expressing RIIS96D *versus* RIIS96A. Expression of recombinant RII constructs showed significant effects on cytosolic calcium transients. We propose a model illustrating a central role of RII phosphorylation in the regulation of local PKA activity. We conclude that RII phosphorylation regulates PKA-dependent substrate phosphorylation and may have significant implications for modulation of cardiac function.

The cAMP-dependent protein kinase (PKA)[2] is a serine/threonine kinase with a prominent role in the regulation of cardiac function. The inactive holoenzyme is composed of a regulatory subunit (R) dimer and two catalytic subunits (PKA_{cat}). The active site of PKA_{cat} reversibly associates with the inhibitory domain of the R subunit. Cooperative binding of cAMP molecules to the four nucleotide binding sites on the R subunit dimer causes dissociation of the PKA_{cat} and, thus, activation of the enzyme (1). However, dissociation of the R and PKA_{cat} subunits may not always occur during activation (2, 3). It is widely known that perturbations of PKA activity, including altered PKA phosphorylation of ryanodine receptor, phospholamban, myosin-binding protein C, and troponin I, occur in the failing heart and may contribute to impaired contractile function (4–8). Decreased phosphorylation of RII is observed during heart failure; however, the mechanisms involved are poorly understood (9). This study will focus on the functional significance of alterations in the phosphorylation state of the RII subunit.

A-kinase-anchoring proteins (AKAPs) bind RII dimers and sequester inactive PKA holoenzyme near its substrates, facilitating phosphorylation of local PKA substrates. Sequence differences among AKAPs result in the assembly of a varied range of signaling molecules targeted to each AKAP (10). For example, mAKAP, which targets PKA to the junctional sarcoplasmic reticulum, binds RII, protein phosphatase 2A, phosphodiesterase 4D3, and ryanodine receptor (11, 12). AKAP15/18α localizes PKA to L-type Ca^{2+} channels. The δ isoform of AKAP15/18 was recently shown to target PKA to phospholamban (13), and phosphodiesterase 3 associates with sarcoplasmic reticulum membranes (14). Thus each AKAP and its associated signaling molecules constitute a unique multifunctional signaling complex.

Ser-96 of RII is located within the RII inhibitory domain and interacts with the catalytic cleft of PKA_{cat} (1). PKA_{cat} phospho-

* This work was supported, in whole or in part, by National Institutes of Health Grants AG16613 and HL79134 (to M. B.). The costs of publication of this article were defrayed in part by the payment of page charges. This article must therefore be hereby marked "*advertisement*" in accordance with 18 U.S.C. Section 1734 solely to indicate this fact.

[S] The on-line version of this article (available at http://www.jbc.org) contains supplemental Figs. S1 and S2.

[1] To whom correspondence should be addressed: Dept. of Physiology, School of Medicine, University of Maryland Baltimore, 655 W. Baltimore St, Baltimore, MD 21201. Tel.: 410-706-1922; Fax: 410-706-8341; E-mail: mbond@som.umaryland.edu.

[2] The abbreviations used are: PKA, cAMP-dependent protein kinase; AKAP, A-kinase-anchoring proteins; RII, regulatory subunit of PKA type II; PKA_{cat}, catalytic subunit of PKA; IBMX, 3-isobutyl-1-methylxanthine; 8-Br-cAMP, 8-bromo-cAMP monophosphate sodium; NCM, neonatal cardiomyocytes; ACM, adult cardiomyocytes; RyR, ryanodine receptor; PLN, phospholamban; SERCA, sarco-endoplasmic reticulum Ca^{2+} ATPase; CSQ, calsequestrin; NCX, Na^+/Ca^{2+} exchanger; WT, wild type; PBS, phosphate-buffered saline; GFP, green fluorescent protein; GAPDH, glyceraldehyde-3-phosphate dehydrogenase.

rylates RII at Ser-96 (15). *In vitro* studies have shown that RII phosphorylation at Ser-96 not only regulates interaction with PKA_{cat} (16, 17), but also affects interaction with AKAPs (18). Studies using PKA purified from bovine cardiac muscle showed that RII phosphorylation increases cAMP-induced dissociation of the PKA holoenzyme, leading to activation of the kinase (19). Our surface plasmon resonance spectroscopy studies showed that phosphorylation of the RII subunit alters the affinity of RII for peptides encompassing the RII binding domains of AKAP15/18, mAKAP, and AKAP-Lbc, with the greatest increase observed for AKAP15/18 (18).

Because phosphorylation of RII can potentially affect both holoenzyme formation and subcellular localization via AKAPs, we investigated whether the phosphorylation state of RII regulates PKA signaling in cardiomyocytes. We created RII fusion proteins that mimic constitutively phosphorylated and non-phosphorylated RII and tested the hypothesis that RII phosphorylation modulates holoenzyme formation, PKA-AKAP interactions, and downstream substrate phosphorylation in intact myocytes. Altered phosphorylation of key PKA substrates then affects cardiomyocyte Ca^{2+} cycling.

Given previous observations that RII phosphorylation is reduced during heart failure (9), this would imply decreased AKAP-mediated subcellular localization of PKA in myocytes of failing hearts, which may then contribute to decreased PKA protein phosphorylation and impaired contractility in heart failure.

EXPERIMENTAL PROCEDURES

Adenovirus Construction—Three different RII constructs (RII*) were created and fused to ECFP. The plasmid for WT RII was previously described (20). To create the S96A, or the S96D mutation in the RII protein, the Stratagene Quick Change XI Site-directed mutagenesis kit was used. Constructs were verified by DNA sequencing. cDNAs encoding WT RII, RIIS96A, and RIIS96D were cloned into the shuttle vector pAdlox. The adenovirus was prepared by Cre-lox recombination (21) with reagents provided by the NIH/NHLBI sponsored Viral core Reagent Program at the University of Pittsburgh.

Cell Culture and Adenoviral Infection—Neonatal and adult cardiomyocytes were isolated as described (22, 23). Neonatal myocytes were cultured in Dulbecco's modified Eagle's medium F12 (ATTC) supplemented with 5% horse serum, (Cambrex), 0.04% bovine serum albumin, (Sigma), 1× insulin-transferrin-selenium (Invitrogen) at 37 °C, 5% CO_2. Neonatal cardiomyocytes were plated at a density of $\sim 6-7 \times 10^6$ cells in a 100-mm laminin-coated (Invitrogen) Petri dish, (10 μg/ml) or 8×10^5 cells in a 24-mm laminin-coated coverslip. Twenty-four hours after plating, infection was carried out using 4 pfu/cell of adenoviral vector in serum-free Dulbecco's modified Eagle's/F12 media. 2× medium was added to the cells after 60–90 min. The expression of recombinant proteins was analyzed after 48 h.

Adult rat cardiomyocytes were plated on laminin-coated dishes (10 μg/ml) and cultured for 2 h in M199 with Hanks Salt (Invitrogen) supplemented with 25.99 mM $NaHCO_3$, 1× insulin-transferrin-selenium (Invitrogen), penicillin (100 units/ml), streptomycin (0.17 mM) (Invitrogen), 5 mM taurine (Sigma), 5 mM creatine (Sigma), 5 mM L-carnitine (Sigma), 5% fetal bovine serum, pH 7.

Fluorescence Microscopy—Cells were fixed with 4% paraformaldehyde in PBS. The cells were placed in 0.1% Triton-X in PBS for 7 min and then incubated in 3% BSA in PBS. Primary antibodies (anti-RII from Upstate and PKA_{cat} from BD) were diluted 1:100 and incubated for 1 h at room temperature. Alexa 488 donkey anti-goat or Alexa 568 donkey anti-mouse (Molecular Probes) was used as a secondary antibody, incubated for 45 min. After extensive washing, the cells were mounted on a slide using Vectashield mounting media (Vector Laboratories, Inc.). Images were collected using a Nikon TE2000U inverted fluorescent microscope equipped with a Spot digital camera and appropriate filters (Diagnostic Instruments, Inc).

Calcium Imaging—Fluorescence imaging was carried out using an Olympus IX50 inverted microscope (×40 objective) equipped with a Roper Cool Snap HQ CCD camera. Cells were loaded for 20 min with 10 μM fluo4-AM (Invitrogen) and washed in Krebs Ringer Buffer (KRB; 125 mM NaCl, 5 mM KCl, 1 mM Na_3PO4, 1 mM $MgSO_4$, 5.5 mM glucose, 20 mM HEPES, pH 7.4) supplemented with 1 mM $CaCl_2$ for an additional 20 min. The coverslip with cells was placed on the stage of an inverted microscope and perfused with KRB supplemented with 1 mM $CaCl_2$. Cells were perfused with 0.5 mM EGTA for 30 s and subsequently stimulated with 10 mM caffeine in 0.5 mM EGTA and imaged at room temperature at ~7 Hz using IPLab software (BD Bioscience). Fluorescence images were normalized to basal levels and reported as F/F_0. The value of the time constant t was calculated by fitting the recovery phase of the fluorescence curve, using the equation $y = y_o + Ae^{-x/t}$.

PKA Activation in Cultured NCM and ACM—Control neonatal myocytes were stimulated either with forskolin, IBMX, 8-Br-cAMP, isoproterenol, or a combination of these agents. Cells were washed in KRB supplemented with 1 mM $CaCl_2$ and then incubated with 25 μM forskolin alone, or together with 100 μM IBMX in KRB/$CaCl_2$ for 5 min at 37 °C, 5% CO_2. Alternatively PKA was activated by incubation with 2.5 nM isoproterenol (alone or together with 100 μM IBMX) in KRB/$CaCl_2$ or 100 μM 8-Br-cAMP for 5 min. All chemicals were from Sigma. Control cells were washed and placed in the incubator with KRB/$CaCl_2$ for 5 min. In experiments with phosphatase inhibitor, 10 nM calyculin A (Calbiochem) was preincubated with the cells for 10 min and maintained at the same concentration during the stimulation. Adult cardiomyocytes were stimulated with 25 μM forskolin, 1 mM 8-Br-cAMP, 1 μM isoproterenol, 100 μM IBMX, or a combination of them in KRB/$CaCl_2$ as indicated. The cells were subsequently lysed in M-PER buffer (Pierce) with protease inhibitors (Sigma), and proteins analyzed via Western blot.

Immunoprecipitation Assay—Neonatal cardiomyocytes were rinsed in PBS and scraped from the plate in M-PER lysis buffer (Pierce) containing protease inhibitors (Sigma), 48-h postinfection. True blot anti-goat IgG IP beads (50 μl) (eBioscience) were added to 700 μg of lysate from cell extracts and incubated for 30 min on ice. After spinning at 10,000 × g for 3 min, the supernatant was separated and incubated with 5 μg of RII antibody. After rocking for 1 h at 4 °C, 50 μl of IgG IP beads were

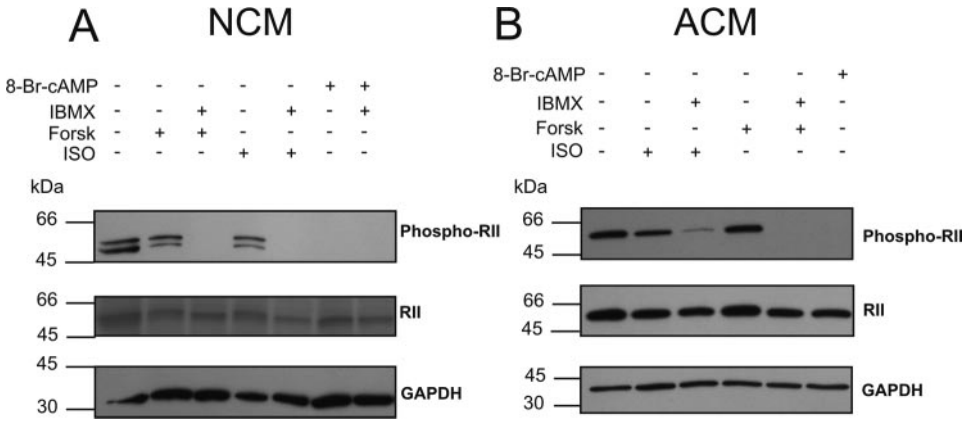

FIGURE 1. **Phosphorylation of endogenous RII protein following activation of PKA in cardiomyocytes.** *A*, NCM were treated for 5 min with forskolin (*Forsk*), isoproterenol (*ISO*), 8-Br-cAMP, or a combination of forskolin or isoproterenol with IBMX, as indicated. Phospho-RII was present at basal conditions and after stimulation with forskolin or isoproterenol alone (*lanes 2* and *4*). A loss of phosphorylated RII was observed in forskolin/IBMX-, isoproterenol/IBMX-, 8-Br-cAMP-, and 8-Br-cAMP/IBMX-treated cells (*lanes 3*, *5*, *6*, and *7*) ($n = 5$). *B*, adult cardiomyocytes (*ACM*) were treated for 5 min as indicated. Maintained activation of PKA also resulted in loss of the phospho-RII band. The *lower panels* show total RII expression and GAPDH staining.

added and incubated for 1 h at room temperature. The immunocomplex beads were washed three times in PBS, incubated in sample buffer, and loaded in a 4–15% gradient SDS-PAGE for immunoblotting.

Western Blot Analysis—The amount of proteins was determined in duplicate, using the Micro BCA Protein Assay kit (Pierce). Proteins (40 μg per lane) were separated by SDS-PAGE using 4–15% gradient or 5% gels (Bio-Rad), then transferred to polyvinylidene difluoride membrane for probing with appropriate antibodies. Quantitative analysis of the bands was performed by densitometry using the Kodak MI Molecular Imaging software (Kodak Molecular Imaging Systems).

The antibodies used were the following: a custom anti-AKAP15-GST polyclonal antibody (a kind gift from Dr. Catterall, University of Washington, Seattle, WA), Phospho-phospholamban Ser-16 and Phospho-ryanodine receptor 2809 (Badrilla, UK), anti-phospholamban and anti-RII (Upstate), anti-ryanodine receptor, SERCA, and calsequestrin (Affinity Bioreagent), anti- Na^+/Ca^{2+} exchanger (Swant, Switzerland), phospho-RII (Epitomics). Horseradish peroxidase-conjugated anti-mouse, anti-goat, or anti-rabbit were used as secondary antibodies (KPL). The True Blot System was used as a secondary antibody in the immunoprecipitation experiments, according to the manufacturer's instructions.

Statistical Analysis—Results are expressed as means ± S.E. Significance was estimated using one-way analysis of variance (ANOVA) across multiple groups. If the data did not conform to a normal distribution, the Kruskal-Wallis one-way ANOVA analysis on ranks was performed. A p value ≤ 0.05 was considered statistically significant.

RESULTS

Effect of β-Adrenergic Stimulation on RII Phosphorylation—The phosphorylated form of RII has been well characterized *in vitro* in purified cardiac and smooth muscle tissue. It has been proposed that RII exists primarily in the phosphorylated form *in vivo* (16, 18, 24). To investigate whether the extent of phosphorylation of RII undergoes changes in intact cardiomyocytes upon β-adrenergic stimulation, we investigated the phosphorylation of endogenous RII (Ser-96) at baseline and under agonist-stimulated conditions in primary rat neonatal and adult cardiomyocytes. In neonatal myocytes (Fig. 1*A*), phosphorylation of RII was observed under baseline conditions (*lane 1*). When myocytes were stimulated with either forskolin or isoproterenol, alone, no significant change in RII phosphorylation *versus* baseline was observed ($n = 5$). However when myocytes were stimulated with forskolin or isoproterenol, in combination with the phosphodiesterase inhibitor, IBMX, we observed loss of the phosphorylated RII band. Stimulation with the cell-permeant, phosphodiesterase-resistant cAMP analogue, 8-Br-cAMP, mimicked this latter effect ($n = 5$). Similar results were obtained when adult cardiomyocytes were stimulated in the same manner, thus indicating that these findings are not specific to neonatal myocytes ($n = 4$, Fig. 1*B*): phospho-RII was present after stimulation of adult cardiomyocytes with isoproterenol alone or forskolin alone (*lanes 2* and *4*); however, the phospho-RII band disappeared after treatment of cells with forskolin/IBMX or 8-Br-cAMP (*lanes 5* and *6*). Phospho-RII was markedly reduced in 2 of 4 experiments where adult cells were treated with isoproterenol/IBMX (*lane 3*) and was absent in the other two experiments.

In neonatal cardiomyocytes, we consistently observed a doublet for phospho-RII, at 55–57 kDa. The lower molecular weight band was also responsive to IBMX. This band may be a developmentally regulated splice variant of RII not present in adult myocytes. The RII phosphoband reappeared when calyculin A (phosphatase inhibitor) was added to the combination of forskolin/IBMX, but treatment of neonatal myocytes with calyculin A alone did not affect the presence of the phosphoband (supplemental Fig. S1). Stimulation of neonatal myocytes with the combination of isoproterenol and calyculin A did not affect the RII phosphoband.

These findings suggest that RII is phosphorylated in cardiomyocytes under baseline conditions. The results are consistent with previous reports in vascular smooth muscle (24) and indicate that upon transient elevation of cAMP, (absence of IBMX) Ser-96 is protected from the action of phosphatases. In contrast, maintained activity of cAMP, by inhibition of cAMP breakdown or the use of 8-Br-cAMP, may result in dissociation of RII and PKA_{cat} and thus permit dephosphorylation of the RII subunit by calyculin A-sensitive phosphatases.

Expression and Characterization of RII Phosphomimics in Neonatal Cardiomyocytes—A widely used approach to mimic phosphorylated or unphosphorylated residues of a protein is mutation of the phosphorylatable Ser/Thr to Asp (or Glu) or Ala, respectively (25, 26). To determine the functional effects of altered RII phosphorylation in cardiac cells, we produced three

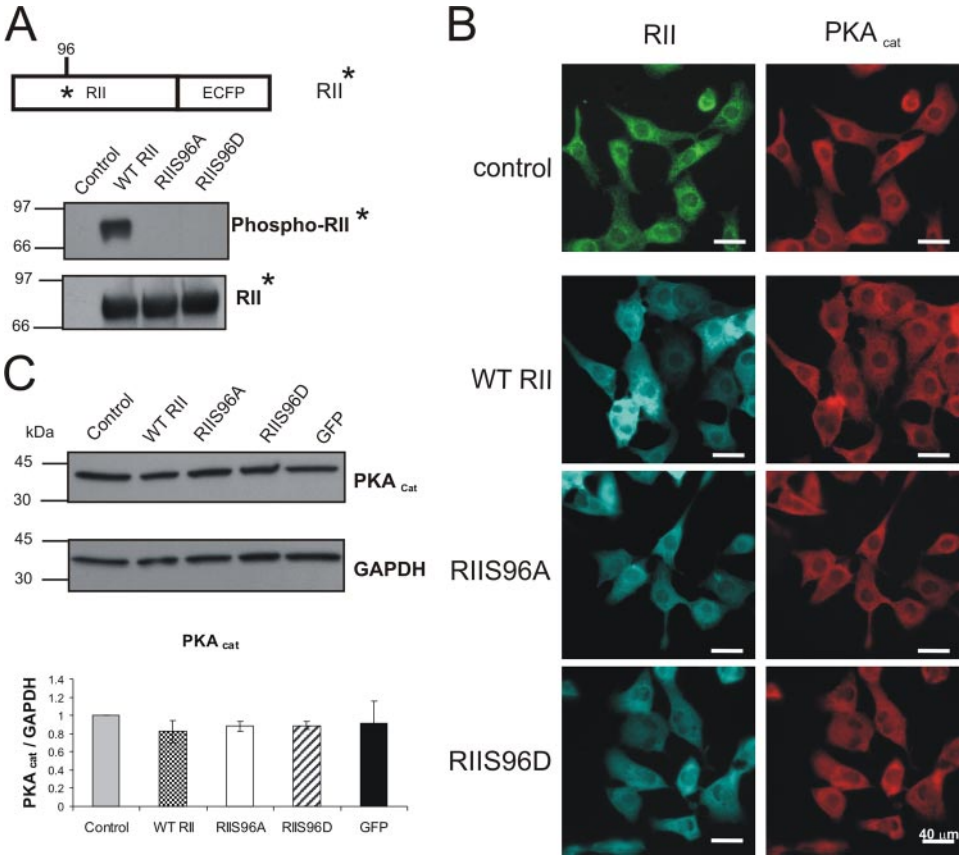

FIGURE 2. **Expression and localization of RII* fusion proteins and PKA_{cat} in NCM.** *A*, schematic diagram shows the design of the RII fusion proteins (RII*) wherein Ser-96 is kept as wild-type (WT RII) or mutated to an alanine (RIIS96A) or aspartate (RIIS96D). Western blot in *A* shows expression of the RII* fusion proteins. The higher molecular mass (~82 kDa) of RII*, relative to endogenous RII, reflected the addition of the ECFP tag. A phospho-RII antibody recognized the phosphorylated WT RII construct. *B*, *upper panel*: control non-infected NCM were probed with antibodies for RII (*left*) and PKA_{cat} (*right*). *B*, *lower panel*: ECFP fluorescence shows cells expressing RII* fusion proteins as indicated (*left*). The same cells were probed with PKA_{cat} antibody (*right*). *Bars*, 40 μm. *C*, representative Western blot showing abundance of PKA_{cat} in control and infected NCM. *Bar graph* indicates unchanged level of PKA_{cat} ($n = 4$).

adenoviral vectors, encoding wild-type RII and two mutants that mimic constitutively phosphorylated (RIIS96D, Ser-96 mutated to Asp) and unphosphorylated (RIIS96A, Ser-96 mutated to Ala) RII. Fig. 2*A* shows a schematic diagram of the RII fusion proteins (RII*). Western blot using the phospho-RII antibody revealed a band of ~82 kDa, corresponding to the molecular mass of recombinant phospho-RII* with ECFP tag, only in cells overexpressing the wild-type RII construct. The observed phosphorylation of recombinant wild-type RII further indicated that RII is phosphorylated under basal conditions. The phosphoantibody did not detect RIIS96A and RIIS96D because of the point mutations in Ser-96.

Fig. 2*B* (*upper panel*) shows non-infected neonatal myocytes immunostained with antibodies to detect endogenous RII and PKA_{cat}. The two PKA components co-localized throughout the cytoplasm and perinuclear region. Immunofluorescence and immunoblotting were performed to determine whether overexpression of RII* constructs altered localization and/or abundance of PKA_{cat} (Fig. 2, *B*, *lower panels* and *C*). In Fig. 2*B* (*lower panel*), the fluorescence of the ECFP tag was used to identify neonatal cells expressing the three RII* fusion proteins. Infection efficiency was 95%. Overexpressed proteins localized throughout the cytoplasm. The second column shows PKA_{cat} expression in the same cells. The intensity of excitation and duration of exposure were kept identical between control and infected cells. No gross differences in localization of PKA_{cat} were noted. Lysates from neonatal myocytes expressing recombinant RII* proteins were analyzed for PKA_{cat} by Western blot (Fig. 2*C*). Neonatal cells infected with adenovirus carrying GFP alone served as an additional control. No significant changes in the abundance of PKA_{cat}, compared with control or to cells expressing GFP, were observed ($n = 4$). Therefore, despite a significant increase in RII*, as a result of expression of recombinant RII* proteins, total PKA_{cat} remained unchanged.

Prior *in vitro* studies showed that phosphorylation of RII (Ser-96), reduced RII affinity for PKA_{cat} ~10-fold (16, 17). If RIIS96D and RIIS96A are valid mimetics of phosphorylated and unphosphorylated RII, respectively, then we should observe decreased binding of PKA_{cat} to expressed RIIS96D *versus* RIIS96A. We compared the amount of PKA_{cat} which co-immunoprecipitated with RIIS96D *versus* RIIS96A. Significantly less PKA_{cat} bound RIIS96D compared with RIIS96A (supplemental Fig. S2), thus, confirming that our constructs are appropriate mimics of phosphorylated and unphosphorylated RII (Ser-96).

Effects of RII Phosphomimics on RII-AKAP Interactions in Cardiomyocytes—AKAP15/18α is a prominent AKAP expressed in cardiomyocytes (27, 28). Recent evidence also reveals expression of AKAP15/18δ in cardiomyocytes (13). Surface plasmon resonance experiments have shown that the affinity of the RII binding region of AKAP15/18 for RII significantly increases when Ser-96 of RII is phosphorylated (18). We therefore investigated whether more AKAP15/18 is co-immunoprecipitated by RIIS96D compared with RIIS96A.

We first confirmed that we had equal protein expression of recombinant RII* and AKAP15/18α under all experimental conditions (Fig. 3*A*). RII antibody coupled to anti-goat IgG IP beads was used to co-immunoprecipitate AKAP15/18 (Fig. 3*B*). The amount of AKAP15/18α immunoprecipitated with each RII* construct (*upper panel*) was normalized to immunoprecipitated recombinant RII* (*bottom panel*). Significantly less AKAP15/18α co-immunoprecipitated with the non-phosphorylated RII mimic RIIS96A, compared with the constitutively phosphorylated mimic RIIS96D or wild-type RII ($p < 0.05$, $n = 5$). Similar results were obtained when the recombinant RII*s were immunoprecipitated with anti-GFP antibody, to avoid

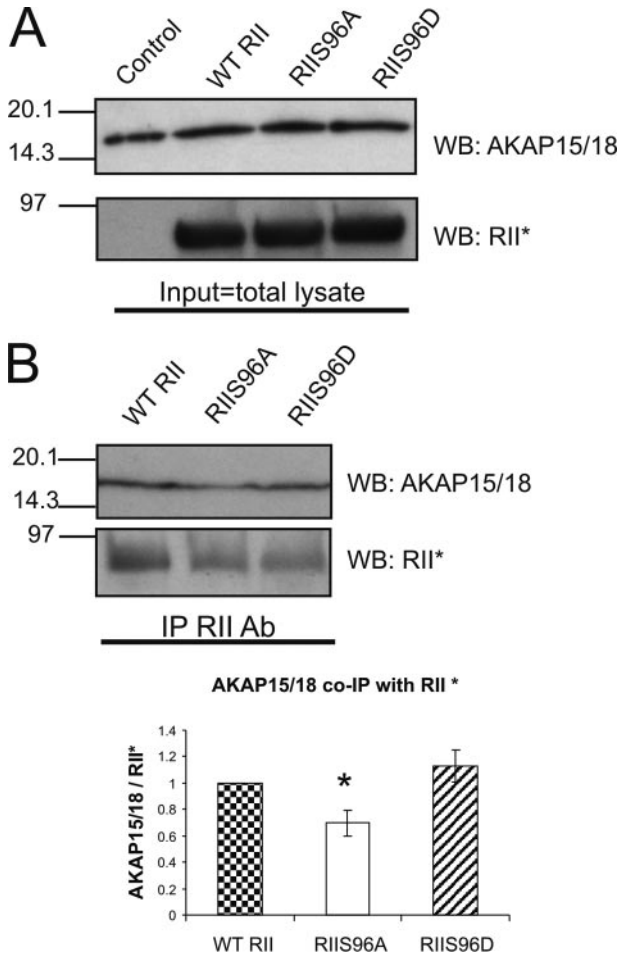

FIGURE 3. **Co-immunoprecipitation of AKAP15/18α with RII* fusion proteins in neonatal cardiomyocytes.** *A*, total cell lysate from control non-infected and NCM expressing RII* fusion proteins were probed with AKAP15/18α and RII antibody to demonstrate equal expression. *B*, co-immunoprecipitation using RII antibody shows that less AKAP15/18α was co-immunoprecipitated with RIIS96A relative to RIIS96D or WT RII. *Bar graph* summarizes results ($n = 5$, *, $p < 0.05$). *Error bars* indicate S.E.

contribution of endogenous RII (data not shown). Consistent with our earlier studies, the results indicate that PKA-AKAP15/18 interaction is significantly increased when RII is phosphorylated at serine 96; thus, suggesting that this may be a mechanism by which PKA-AKAP interactions are regulated *in vivo*.

Effects of RII Phosphomimic on PKA Substrate Phosphorylation—To test the hypothesis that altered RII-AKAP binding (via expression of phosphorylation mutants) regulates local PKA activity, we measured phosphorylation of two key PKA substrates: ryanodine receptor and phospholamban (29). The amount of ryanodine receptor and phospholamban showed no significant difference between cells expressing recombinant RII* proteins (or GFP), compared with uninfected control (Fig. 4, *A* and *C*). Under basal conditions, the fraction of phosphorylated ryanodine receptor/total ryanodine receptor was significantly greater in neonatal cells expressing the phosphorylated mimic RIIS96D, compared with RIIS96A, wild-type RII, uninfected controls, ($n = 5$, $p < 0.05$), or GFP controls ($n = 3$, $p < 0.05$) (Fig. 4*B*). Similarly the fractional content of phosphorylated phospholamban was significantly greater in neonatal myocytes expressing RIIS96D, compared with RIIS96A ($n = 4$, $p < 0.05$) (Fig. 4, *C* and *D*). Interestingly, we also noted that basal phosphorylation of phospholamban was significantly reduced in wild-type RII and RIIS96A-expressing cells, relative to uninfected myocytes ($n = 4$, $p < 0.05$).

The relative increase in PKA-dependent phosphorylation of both ryanodine receptor and phospholamban, in cells expressing the phosphorylated mimic RIIS96D *versus* the non-phosphorylated mimic RIIS96A further supports the hypothesis that increased phosphorylation of RII (RIIS96D phosphorylated mimic) results in increased PKA binding to AKAPs, PKA localization near its substrates, and PKA-dependent substrate phosphorylation.

Effects of RII Phosphomimics on Ca^{2+} Homeostasis—We first investigated whether adenoviral expression affected levels of Ca^{2+} regulatory proteins. We measured abundance of SERCA, calsequestrin, and Na^+/Ca^{2+} exchanger protein (Fig. 5). The amount of calsequestrin ($n = 7$) and Na^+/Ca^{2+} exchanger protein ($n = 5$) remained unchanged in all three groups of cells expressing RII* constructs, compared with uninfected controls or cells infected with GFP alone. However, SERCA was significantly reduced in all three experimental groups of cells expressing recombinant RII* constructs, compared with uninfected controls or cells expressing GFP ($n = 4$, $p < 0.05$) (Fig. 5*B*). The decrease in expression of SERCA was not due to adenoviral infection *per se*, because those cells infected with GFP (similar to CFP) did not demonstrate a decrease in SERCA.

We then used the Ca^{2+} indicator Fluo4 to determine the effect of expression of RII* on spontaneous Ca^{2+} oscillations, in the presence of 1 mM extracellular Ca^{2+}. Frequency of spontaneous activity was similar in control and infected neonatal cardiomyocytes (median values (number of events/30 s): control = 6.5, wild-type RII = 5, RIIS96A = 5, RIIS96D = 6). However, the time course of Ca^{2+} oscillations is regulated by several Ca^{2+} transport pathways: release of Ca^{2+} from the sarcoplasmic reticulum, sarcolemmal Ca^{2+} influx, Ca^{2+} reuptake into the sarcoplasmic reticulum, and sarcolemmal Ca^{2+} efflux. We then isolated the sarcoplasmic reticulum Ca^{2+} release component of the Ca^{2+} transient by stimulating the myocytes with caffeine, under Ca^{2+}-free conditions. Because we observed that SERCA protein was decreased under all conditions where RII* constructs were expressed (Fig. 5), this was likely to cause decreased availability of releasable Ca^{2+} from the SR as a result of reduced SERCA-dependent Ca^{2+} uptake. Fig. 6*A* shows a representative Ca^{2+} fluorescence trace for each experimental condition.

Interestingly, despite a significant reduction in SERCA protein expression compared with uninfected controls (Fig. 5*A*), the median peak Fluo4 fluorescence was not significantly reduced in RIIS96D cells (1.43, $n = 117$) *versus* controls (1.47, $n = 120$) (Fig. 6*B* and Table 1). In contrast, the median peak fluorescence was significantly reduced in cells expressing RIIS96A (1.39, $n = 143$) and in cells expressing wild-type RII (1.22, $n = 70$), compared with control (cells derived from seven separate cell isolations). These results indicate that the caffeine-releasable Ca^{2+} store is decreased in neonatal myocytes expressing the non-phospho-mimic, RIIS96A (or wild-type RII), compared with uninfected controls.

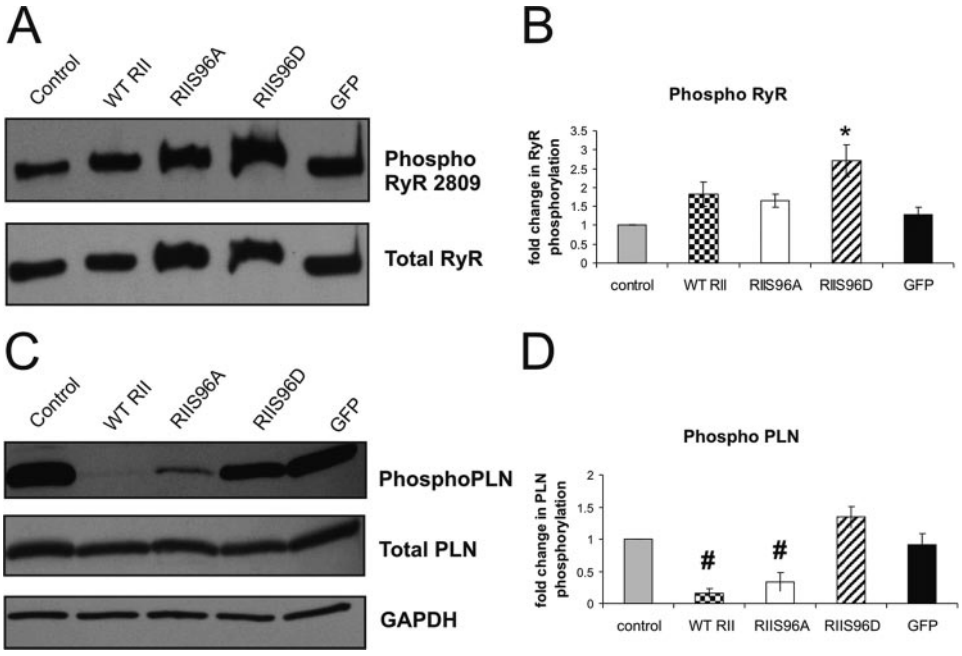

FIGURE 4. **Phosphorylation of RyR and PLN in NCM expressing recombinant RII* proteins.** *A*, blot containing cell lysate from control non-infected NCM and NCM expressing recombinant RII* fusion proteins or GFP was probed with antibody for phosphorylated ryanodine receptor (phospho-RyR Ser-2809), and total RyR, as indicated. *B*, *bar graph* shows that phospho-RyR was significantly increased in cells expressing RIIS96D, *versus* RIIS96A, WT RII, and non-infected cells ($n = 5$, *, $p < 0.05$). *C*, blot was probed with anti-phosphorylated phospholamban (phospho-PLN, Ser-16) and total PLN antibody. GAPDH staining shows equal loading. *D*, summary shows that the level of phospho-PLN was significantly reduced in cells expressing WT RII and RIIS96A compared with RIIS96D and non-infected control ($n = 4$, #, $p < 0.05$). *Error bars* indicate S.E.

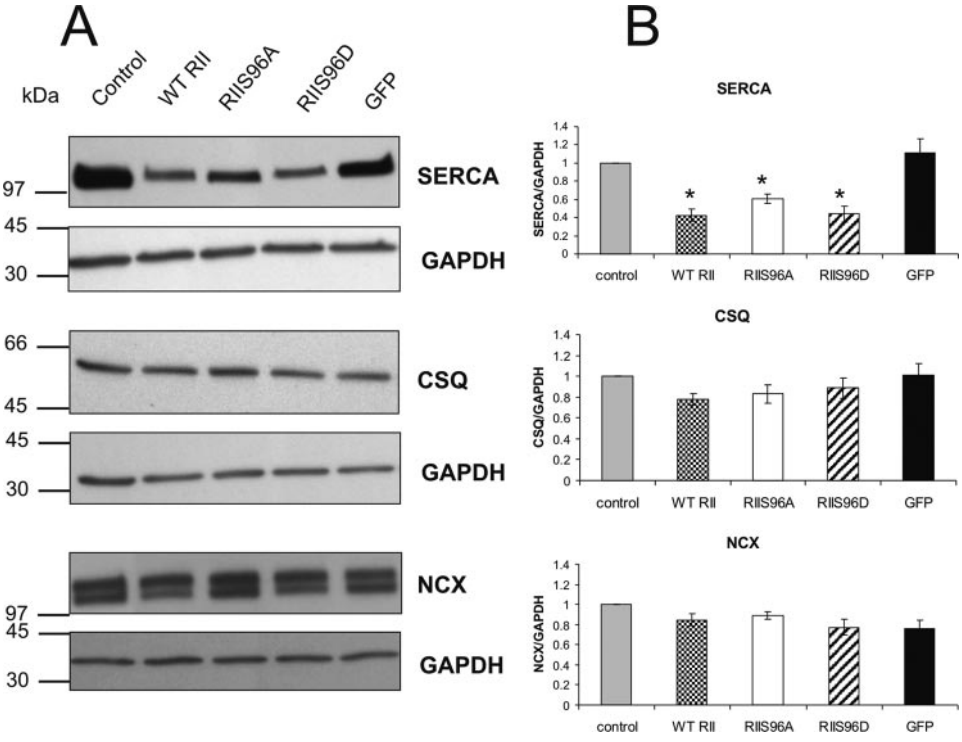

FIGURE 5. **Abundance of SERCA, calsequestrin, and Na^+/Ca^{2+} exchanger in NCM expressing RII* recombinant proteins.** *A*, representative Western blot of control non-infected and NCM infected with RII* constructs or GFP. The blots were probed with antibodies as indicated. Staining for GAPDH verified equal loading. *B*, *bar graphs* summarize results. NCM infection with RII* fusion proteins resulted in a significant reduction of SERCA ($n = 4$) compared with control (*, $p < 0.05$), but did not change calsequestrin (*CSQ*) ($n = 7$) or Na^+/Ca^{2+} exchanger (*NCX*) ($n = 5$). *Error bars* indicate S.E.

Interestingly, while we observed a reduction in SERCA protein levels in neonatal cardiomyocytes expressing all RII* constructs, the decay time constant, *t*, of the Ca^{2+} transient was significantly shorter in cells expressing wild-type RII ($t = 3.73$, $n = 61$), RIIS96A ($t = 3.82$, $n = 132$), and RIIS96D ($t = 3.70$, $n = 106$), *versus* uninfected controls ($t = 5.18$, $n = 103$) (Fig. 6*C*).

DISCUSSION

The specificity and efficiency of PKA depend upon its subcellular localization by AKAPs (10). *In vitro* studies have revealed that phosphorylation of RII regulates its binding to both AKAPs and PKA_{cat}. We tested the hypothesis that the phosphorylation state of RII is critical to control of local PKA activity. We used adenoviral infection to express wild-type RII and RII mutants that mimic phosphorylated or nonphosphorylated RII, in neonatal rat cardiomyocytes. Co-immunoprecipitation of AKAP15/18 and the catalytic subunit of PKA confirmed that RIIS96D mimics phosphorylated RII and RIIS96A mimics nonphosphorylated RII. We then demonstrated that the RII phospho- and nonphosphomimics differentially affected phosphorylation of PKA substrates and Ca^{2+} signaling. Overall, our results demonstrate that the phosphorylation state of the RII subunit is a critical factor which regulates (i) AKAP-RII interaction, (ii) PKA substrate phosphorylation, and (iii) Ca^{2+} signaling in rat cardiomyocytes.

RII Phosphorylation Is Dynamically Regulated in Cardiomyocytes—Previous *in vitro* studies suggested that RII is phosphorylated at basal levels (16, 24, 30). We have now shown, for the first time, the effect of elevated cAMP on the phosphorylation state of RII in cardiomyocytes. We show that stimulation of neonatal or adult cardiomyocytes with forskolin or isoproterenol, in combination with IBMX, to maintain elevated cAMP, eliminates RII phosphorylation. This result contrasts with the increase in phospho-

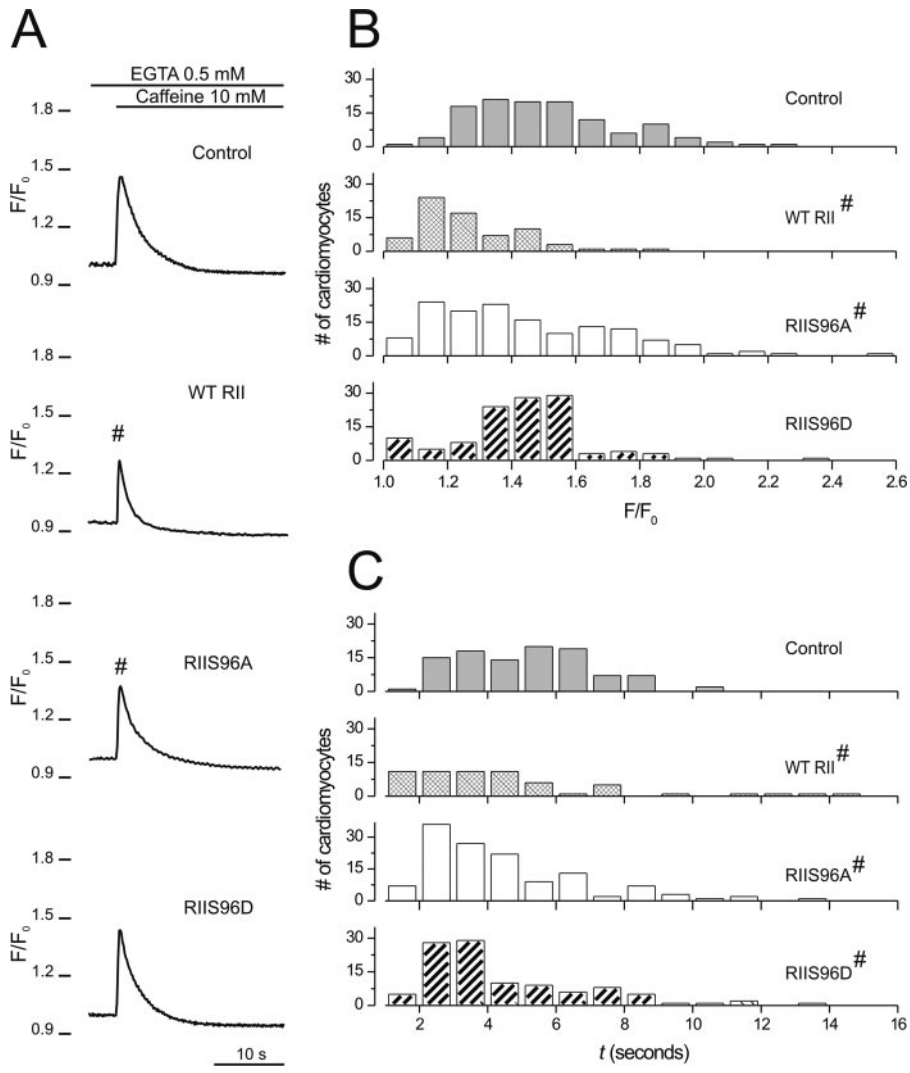

FIGURE 6. **Caffeine-induced calcium transient in NCM expressing RII* recombinant proteins.** *A*, cells were stimulated with caffeine under Ca^{2+}-free conditions. All traces were normalized to baseline value (F_0) and reported as F/F_0. Fluorescence traces are representative of at least 70 independent cells for each condition from a total of 7 different cell isolations. *B* and *C* show the frequency distribution of caffeine-induced Ca^{2+} peak fluorescence and decay time constant *t*, respectively. The median Ca^{2+} peak fluorescence was significantly reduced in cells expressing RIIS96A and WT RII compared with control non-infected NCM) (#, $p < 0.05$), but was unchanged in RIIS96D. The decay time constant *t* was significantly lower in cells expressing wild-type RII, RIIS96A, and RIIS96D, *versus* uninfected controls (#, $p < 0.05$).

TABLE 1

Summary of effects of expression of RII mutants, RIIS96D and RIIS96A, relative to uninfected controls

	RIIS96D	RIIS96A
Phospho-RyR	↑	=
Phospho-PLN	=	↓
Ca^{2+} release	=	↓

rylation observed with other PKA substrates (*e.g.* phospholamban, ryanodine receptor, troponin I), which show a dramatic increase in phosphorylation as a result of increased cAMP. These findings are consistent with *in vitro* studies where addition of cAMP caused RII dephosphorylation in purified bovine cardiac muscle strips or tracheal smooth muscle (30).

In contrast, myocytes stimulated with forskolin or isoproterenol alone (Fig. 1, *A*, *lanes 2* and *4* and *B*, *lanes 2* and *4*) did not show a significant decrease in RII phosphorylation, as compared with unstimulated myocytes. We conclude that phosphatases have greater access to phosphorylated serine 96 when cAMP is maintained at high levels (IBMX added), and the holoenzyme is fully dissociated. Thus, the phosphorylation state of RII in cardiomyocytes is a function of the activities of not only of PKA_{cat} but also of adenylyl cyclase, phosphodiesterase, and phosphatase(s) associated with each PKA:AKAP signaling microdomain (14, 31).

RII Phosphorylation Regulates AKAP-RII Interaction in Cardiomyocytes—Our previous surface plasmon resonance studies showed that the peptide region encompassing the RII binding domain of AKAP15/18, showed the largest increase in binding affinity for RII when the RII subunit is phosphorylated, compared with other AKAPs tested (18). We therefore chose to study the effects of RII phosphorylation on AKAP-RII interactions with endogenous AKAP15/18 in cardiac myocytes. We observed that the phosphorylated RII mimic (RIIS96D) co-immunoprecipitated more AKAP15/18α relative to the non-phosphomimic, RIIS96A, thus indicating that RII phosphorylation increases RII-AKAP15/18 interaction in cardiomyocytes. The decreased AKAP15/18α binding of RIIS96A is less than observed in our previous surface plasmon resonance studies where we compared AKAP15/18α binding to phosphorylated and unphosphorylated recombinant RII. This difference is likely due to the fact that we used only the 24-amino acid RII binding domain of the AKAP in these earlier studies. Because the sequence of the RII binding domain is the same for all AKAP15/18 isoforms, we also predict increased binding of phosphorylated RII to AKAP15/18δ, which was recently shown to co-immunoprecipitate with phospholamban (13). Overall, our results show that PKA binding to AKAPs is regulated by the phosphorylation state of RII in cardiomyocytes.

RII Phosphorylation Increases PKA Phosphorylation of Ryanodine Receptor and Phospholamban—Consistent with earlier studies, expression of RII* constructs did not alter amounts of PKA_{cat} (32). Thus any change observed in PKA activity, as indicated by altered substrate phosphorylation, cannot be ascribed to altered levels of PKA_{cat}. Because RII phosphorylation can (i) increase binding of RII to AKAPs and (ii) decrease binding of RII-PKA_{cat} (33), we predicted increased PKA substrate phos-

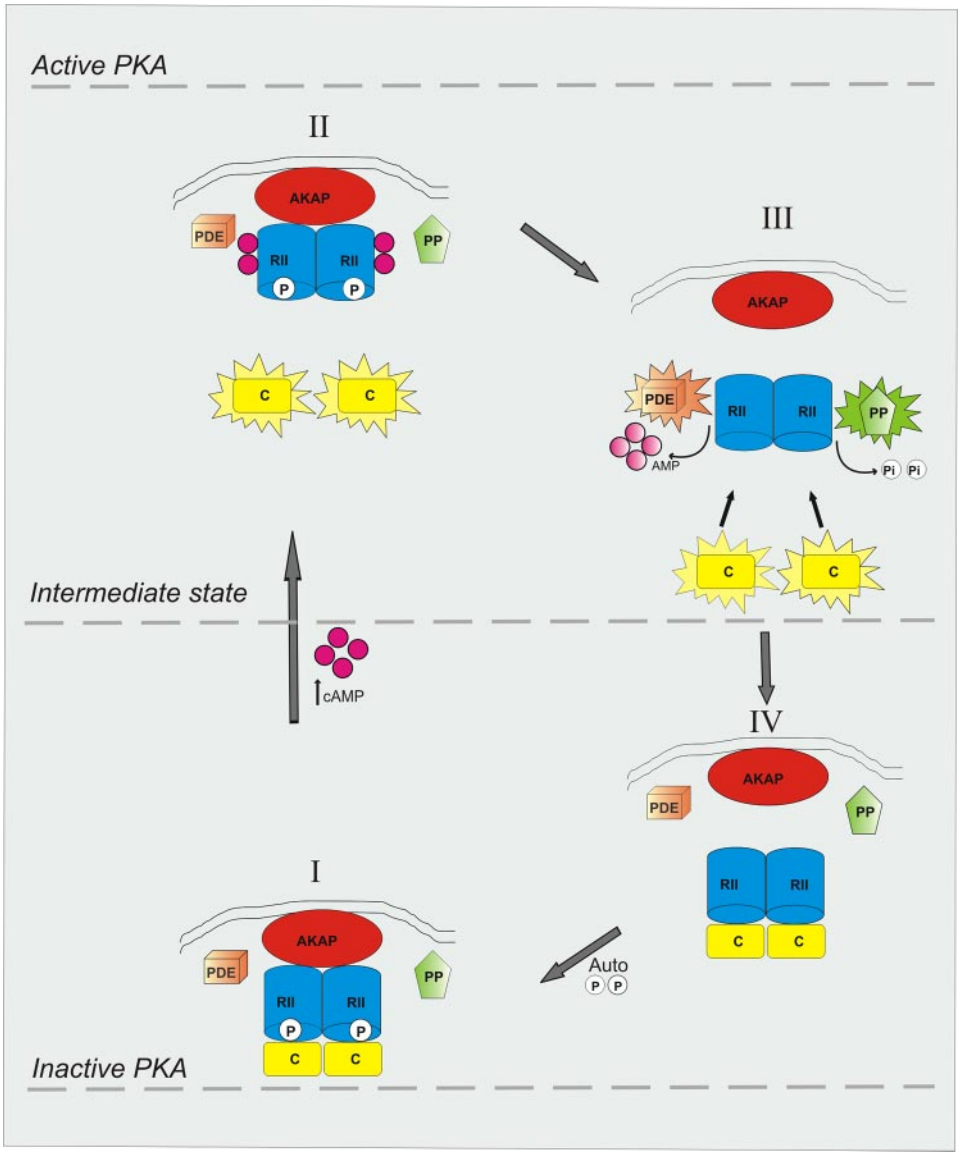

FIGURE 7. **Schematic model of the proposed role of autophosphorylation of RII on AKAP-RII interaction and control of local PKA activity.**

phorylation in cells expressing the phosphomimic RIIS96D *versus* RIIS96A.

In agreement with Xiao *et al.* (34) the present study demonstrated phosphorylation of ryanodine receptor in uninfected cardiomyocytes under non-stimulated conditions. Basal PKA phosphorylation of ryanodine receptor was also observed in neonatal myocytes expressing RII* constructs. In support of our hypothesis, ryanodine receptor phosphorylation was significantly increased in neonatal myocytes expressing RIIS96D, compared with RIIS96A.

Our measurements of phosphorylation of phospholamban showed a similar trend. Consistent with our hypothesis, phosphorylation of phospholamban at Ser-16 was significantly increased in RIIS96D-expressing cells relative to RIIS96A-expressing cardiomyocytes (and uninfected cells). Thus, phosphorylation of ryanodine receptor and phospholamban are significantly increased in cells expressing the phosphorylated RII mimic (RIIS96D), compared with the non-phosphorylated mimic (RIIS96A). These results support the hypothesis that the greater PKA binding to AKAPs and thus increased PKA localization by AKAPs, as a result of increased RII phosphorylation, leads to increased phosphorylation of PKA substrates. Table 1 summarizes the effects of the phosphorylated and non-phosphorylated RII mimics on phosphorylation of PKA substrates. These findings thus demonstrate for the first time that PKA targeting to AKAPs, as modulated by RII phosphorylation, regulates substrate phosphorylation in cardiac myocytes.

Basal phospholamban phosphorylation in neonatal myocytes expressing wild-type RII (Fig. 4, *C* and *D*), was significantly reduced, compared with phospholamban phosphorylation in uninfected controls, although this was not observed with ryanodine receptor phosphorylation. How did such differences in basal phosphorylation of phospholamban and ryanodine receptor occur, as a result of expression of wild-type RII? We offer the following explanation: it is now well established that multienzyme complexes define unique restricted cellular signaling microdomains (35). For example, phosphodiesterases (primarily PDE3 and PDE4) within different subcellular microdomains are reported to have different roles in PKA signaling (12, 36, 37). Because PKA_{cat} levels were unchanged (Fig. 2, *B* and *C*) across all experimental groups, adenoviral expression of wild-type RII results in a ratio of wild-type RII:PKA_{cat} > 1. Thus all wild-type RII molecules will not be phosphorylated by PKA_{cat} at the baseline. Furthermore, given compartmentalization of signaling molecules in cardiac myocytes and differences in local subset concentration and activity of adenylyl cyclases, phosphodiesterases, and phosphatases, steady state RII phosphorylation will differ in different microdomains of the cell. Thus, our observation of decreased phospholamban phosphorylation upon expression of wild-type RII suggests that unphosphorylated RII is enriched in the microdomain around phospholamban.

RII Phosphorylation Modulates Ca^{2+} Signaling—We have shown that expression of RIIS96D *versus* RIIS96A differentially regulates phosphorylation of proteins integral to Ca^{2+} signaling. We hypothesized that expression of RII phosphomimics would also affect dynamics of cytosolic Ca^{2+}. Whereas we observed no significant difference in protein levels of ryanodine

receptor, phospholamban, calsequestrin, and Na^+/Ca^{2+} exchanger in neonatal cardiomyocytes expressing RII* constructs, compared with controls, SERCA levels were significantly reduced. Consistent with decreased SERCA and phospholamban phosphorylation, the amplitude of the caffeine-induced Ca^{2+} transient was decreased in cells expressing RIIS96A, *versus* uninfected controls. These results are consistent with previous findings in transgenic mice overexpressing an unphosphorylated mimic of phospholamban (S16A phospholamban) where contractility and calcium cycling were decreased (38).

In contrast, despite a 56% decrease in SERCA expression in RIIS96D-expressing cells, *versus* uninfected controls, cells expressing RIIS96D showed no decrease in amplitude of the caffeine-induced Ca^{2+} transient and thus no decrease in size of caffeine-releasable Ca^{2+} stores. We conclude that the increased phosphorylation of ryanodine receptor, together with maintained phospholamban phosphorylation, as a result of expression of the phosphorylated RII mimic, compensates for decreased SERCA expression and permits the sarcoplasmic reticulum to store and release Ca^{2+} in amounts comparable to uninfected controls.

Interestingly, neonatal myocytes expressing RII* constructs displayed faster Ca^{2+} decay kinetics than uninfected controls. The rate of decline in cytosolic Ca^{2+} during cardiac relaxation is primarily determined by SERCA, regulated by phospholamban, and by the Na^+/Ca^{2+} exchanger (39, 40). Our Ca^{2+} cycling experiments were conducted in the presence of caffeine and EGTA; thus in our study, Ca^{2+} reuptake into the sarcoplasmic reticulum took place following caffeine depletion of Ca^{2+} from the sarcoplasmic reticulum via the ryanodine receptor, and in the absence of extracellular Ca^{2+}; Ca^{2+} efflux via the Na^+/Ca^{2+} was also facilitated by an outwardly directed Ca^{2+} gradient. Because expression of the Na^+/Ca^{2+} exchanger was unchanged in all groups, altered expression of the exchanger cannot account for the differences observed. The mechanism responsible for the increased rate of decline of cytoplasmic Ca^{2+} in RII*-expressing cells thus remains to be determined.

In heart failure, reduced SERCA expression and phospholamban hypophosphorylation is proposed to result in decreased SERCA activity, reduced peak systolic Ca^{2+}, and prolongation of the Ca^{2+} transient (41–43). However, expression of a pseudophosphorylated phospholamban suppressed heart failure progression in cardiomyopathic hamsters (44). Other studies have shown improved contractility as a result of increased abundance or activity of specific proteins (SERCA, phospholamban, TnI) (45, 46), or enhanced β-adrenergic signaling (47, 48). Such approaches may be promising therapies for heart failure. Whereas the expression of the phosphomimic RIIS96D does not necessarily restore SERCA expression levels, normalization of phospholamban phosphorylation and Ca^{2+} signaling kinetics were observed, and thus expression of a pseudophosphorylated RII could be of potential therapeutic benefit in cardiac syndromes where contractility is depressed because of mutations or hypophosphorylation of phospholamban (8, 49).

CONCLUSION

In summary, our results indicate that the phosphorylation state of the RII subunit affects: 1) RII-PKA_{cat} interactions, 2) RII-AKAP interactions, 3) phosphorylation of PKA substrates, and 4) Ca^{2+} signaling. The results can be modeled by an autoregulatory feedback modulation of PKA activity (Fig. 7): RII subunits within the PKA heterotetramer are phosphorylated at basal levels, (*inactive PKA; stage I*); elevated cAMP binds RII subunits, leading to PKA_{cat} (*C*) release (*active PKA, stage II*): free RII, with increased availability of serine 96 to phosphatases (*PP*) is dephosphorylated; dephosphorylation of RII reduces its affinity for AKAPs but increases its affinity for PKA_{cat} (*intermediate stage III*) (33); decreased cAMP, as a result of phosphodiesterase activity also occurs; the coordinated dephosphorylation of RII and decreased cAMP leads to reformation of PKA holoenzyme (*intermediate stage IV*); autophosphorylation of RII by PKA_{cat} increases affinity for the AKAP and terminates the cycle. In summary, we have provided evidence to support the novel idea that cyclical regulation of phosphorylation of RII (Ser-96) is part of an autoregulatory feedback loop responsible for controlling local activation and termination of PKA activity.

Acknowledgments—We thank Shirley Gaa and Dr. Terry Rogers for providing us with neonatal cardiomyocytes, Dr. Wenhong Xu and Dr. William Stanley for adult cardiomyocytes, Dr. Mary Ruehr and Russ Desnoyer for cDNA containing the S96A and S96D mutations, and Dr. Linda Lund for critical review of the manuscript. We gratefully acknowledge the generous gifts of phospho-PLN antibody from Dr. Evangelia Kranias and anti-AKAP15-GST antibody from Dr. William Catterall.

REFERENCES

1. Taylor, S. S., Buechler, J. A., and Yonemoto, W. (1990) *Annu. Rev. Biochem.* **59,** 971–1005
2. Prinz, A., Diskar, M., Erlbruch, A., and Herberg, F. W. (2006) *Cell Signal.* **18,** 1616–1625
3. Yang, S., Fletcher, W. H., and Johnson, D. A. (1995) *Biochemistry* **34,** 6267–6271
4. Wehrens, X. H., and Marks, A. R. (2004) *Ann. Med.* **36,** Suppl. 1, 70–80
5. Sipido, K. R., and Eisner, D. (2005) *Cardiovasc. Res.* **68,** 167–174
6. Hasenfuss, G. (1998) *Cardiovasc. Res.* **37,** 279–289
7. Bodor, G. S., Oakeley, A. E., Allen, P. D., Crimmins, D. L., Ladenson, J. H., and Anderson, P. A. (1997) *Circulation* **96,** 1495–1500
8. Waggoner, J. R., and Kranias, E. G. (2005) *Heart Fail. Clin.* **1,** 207–218
9. Zakhary, D. R., Moravec, C. S., and Bond, M. (2000) *Circulation* **101,** 1459–1464
10. Ruehr, M. L., Russell, M. A., and Bond, M. (2004) *J. Mol. Cell Cardiol.* **37,** 653–665
11. Kapiloff, M. S., Jackson, N., and Airhart, N. (2001) *J. Cell Sci.* **114,** 3167–3176
12. Dodge-Kafka, K. L., Soughayer, J., Pare, G. C., Carlisle Michel, J. J., Langeberg, L. K., Kapiloff, M. S., and Scott, J. D. (2005) *Nature* **437,** 574–578
13. Lygren, B., Carlson, C. R., Santamaria, K., Lissandron, V., McSorley, T., Litzenberg, J., Lorenz, D., Wiesner, B., Rosenthal, W., Zaccolo, M., Tasken, K., and Klussmann, E. (2007) *EMBO Rep.* **8,** 1061–1067
14. Fischmeister, R., Castro, L. R., Abi-Gerges, A., Rochais, F., Jurevicius, J., Leroy, J., and Vandecasteele, G. (2006) *Circ. Res.* **99,** 816–828
15. Tasken, K., and Aandahl, E. M. (2004) *Physiol. Rev.* **84,** 137–167
16. Rangel-Aldao, R., Kupiec, J. W., and Rosen, O. M. (1979) *J. Biol. Chem.* **254,** 2499–2508
17. Granot, J., Mildvan, A. S., Hiyama, K., Kondo, H., and Kaiser, E. T. (1980) *J. Biol. Chem.* **255,** 4569–4573

18. Zakhary, D. R., Fink, M. A., Ruehr, M. L., and Bond, M. (2000) *J. Biol. Chem.* **275,** 41389–41395
19. Erlichman, J., Rosenfeld, R., and Rosen, O. M. (1974) *J. Biol. Chem.* **249,** 5000–5003
20. Ruehr, M. L., Zakhary, D. R., Damron, D. S., and Bond, M. (1999) *J. Biol. Chem.* **274,** 33092–33096
21. Hardy, S., Kitamura, M., Harris-Stansil, T., Dai, Y., and Phipps, M. L. (1997) *J. Virol.* **71,** 1842–1849
22. Lokuta, A., Kirby, M. S., Gaa, S. T., Lederer, W. J., and Rogers, T. B. (1994) *J. Cardiovasc. Electrophysiol.* **5,** 50–62
23. Tytgat, J. (1994) *Cardiovasc. Res.* **28,** 280–283
24. Scott, C. W., and Mumby, M. C. (1985) *J. Biol. Chem.* **260,** 2274–2280
25. Rodriguez-Vilarrupla, A., Jaumot, M., Abella, N., Canela, N., Brun, S., Diaz, C., Estanyol, J. M., Bachs, O., and Agell, N. (2005) *Mol. Cell Biol.* **25,** 7364–7374
26. Wehrens, X. H., Lehnart, S. E., Reiken, S., Vest, J. A., Wronska, A., and Marks, A. R. (2006) *Proc. Natl. Acad. Sci. U. S. A.* **103,** 511–518
27. Fraser, I. D., Tavalin, S. J., Lester, L. B., Langeberg, L. K., Westphal, A. M., Dean, R. A., Marrion, N. V., and Scott, J. D. (1998) *EMBO J.* **17,** 2261–2272
28. Hulme, J. T., Lin, T. W., Westenbroek, R. E., Scheuer, T., and Catterall, W. A. (2003) *Proc. Natl. Acad. Sci. U. S. A.* **100,** 13093–13098
29. MacLennan, D. H., and Kranias, E. G. (2003) *Nat. Rev. Mol. Cell Biol.* **4,** 566–577
30. Rosen, O. M., and Erlichman, J. (1975) *J. Biol. Chem.* **250,** 7788–7794
31. Zaccolo, M. (2006) *Eur. J. Cell Biol.* **85,** 693–697
32. Otten, A. D., and McKnight, G. S. (1989) *J. Biol. Chem.* **264,** 20255–20260
33. Rangel-Aldao, R., and Rosen, O. M. (1977) *J. Biol. Chem.* **252,** 7140–7145
34. Xiao, B., Zhong, G., Obayashi, M., Yang, D., Chen, K., Walsh, M. P., Shimoni, Y., Cheng, H., Ter Keurs, H., and Chen, S. R. (2006) *Biochem. J.* **396,** 7–16
35. Zaccolo, M., Di Benedetto, G., Lissandron, V., Mancuso, L., Terrin, A., and Zamparo, I. (2006) *Biochem. Soc. Trans.* **34,** 495–497
36. Mongillo, M., McSorley, T., Evellin, S., Sood, A., Lissandron, V., Terrin, A., Huston, E., Hannawacker, A., Lohse, M. J., Pozzan, T., Houslay, M. D., and Zaccolo, M. (2004) *Circ. Res.* **95,** 67–75
37. Rochais, F., Abi-Gerges, A., Horner, K., Lefebvre, F., Cooper, D. M., Conti, M., Fischmeister, R., and Vandecasteele, G. (2006) *Circ. Res.* **98,** 1081–1088
38. Chu, G., Lester, J. W., Young, K. B., Luo, W., Zhai, J., and Kranias, E. G. (2000) *J. Biol. Chem.* **275,** 38938–38943
39. Bers, D. M. (2002) *Nature* **415,** 198–205
40. Trafford, A. W., Diaz, M. E., O'Neill, S. C., and Eisner, D. A. (2002) *Front Biosci.* **7,** d843–52
41. Pieske, B., Maier, L. S., and Schmidt-Schweda, S. (2002) *Basic Res. Cardiol.* **97,** Suppl. 1, I63–I71
42. Houser, S. R., Piacentino, V., 3rd, Mattiello, J., Weisser, J., and Gaughan, J. P. (2000) *Trends Cardiovasc. Med.* **10,** 101–107
43. Dash, R., Frank, K. F., Carr, A. N., Moravec, C. S., and Kranias, E. G. (2001) *J. Mol. Cell Cardiol.* **33,** 1345–1353
44. Hoshijima, M., Ikeda, Y., Iwanaga, Y., Minamisawa, S., Date, M. O., Gu, Y., Iwatate, M., Li, M., Wang, L., Wilson, J. M., Wang, Y., Ross, J., Jr., and Chien, K. R. (2002) *Nat. Med.* **8,** 864–871
45. Miyamoto, M. I., del Monte, F., Schmidt, U., DiSalvo, T. S., Kang, Z. B., Matsui, T., Guerrero, J. L., Gwathmey, J. K., Rosenzweig, A., and Hajjar, R. J. (2000) *Proc. Natl. Acad. Sci. U. S. A.* **97,** 793–798
46. Li, L., Desantiago, J., Chu, G., Kranias, E. G., and Bers, D. M. (2000) *Am. J. Physiol. Heart Circ. Physiol.* **278,** H769–H779
47. Freeman, K., Lerman, I., Kranias, E. G., Bohlmeyer, T., Bristow, M. R., Lefkowitz, R. J., Iaccarino, G., Koch, W. J., and Leinwand, L. A. (2001) *J. Clin. Investig.* **107,** 967–974
48. Eckhart, A. D., and Koch, W. J. (2002) *Mol. Ther.* **5,** 74–79
49. Schmitt, J. P., Kamisago, M., Asahi, M., Li, G. H., Ahmad, F., Mende, U., Kranias, E. G., MacLennan, D. H., Seidman, J. G., and Seidman, C. E. (2003) *Science* **299,** 1410–1413